ANL/RA/CP-103424

Thermal Fatigue Due to Beam Interruptions in a Lead-Bismuth Cooled ATW Blanket*

by

Floyd Dunn

*Work supported by the U.S. Department of Energy, Nuclear Energy Programs under Contract W-31-109-ENG-38.

DISCLAIMER

DISCLAIMER

THERMAL FATIGUE DUE TO BEAM INTERRUPTIONS IN A LEAD-BISMUTH COOLED ATW BLANKET

Floyd Dunn
Argonne National Laboratory
9700 South Cass Avenue
Argonne, Illinois 60439
(630) 252-4692

RECEIVED
DEC 0 8 2000
OSTI

ABSTRACT

Thermal fatigue consequences of frequent accelerator beam interruptions are quantified for both sodium and lead-bismuth cooled blankets in current designs for accelerator transmutation of waste devices. Temperature response was calculated using the SASSYS-1 systems analysis code for an immediate drop in beam current from full power to zero. Coolant temperatures from SASSYS-1 were fed into a multi-node structure temperature calculation to obtain thermal strains for various structural components. Fatigue curves from the American Society of Mechanical Engineers Boiler and Pressure Vessel Code were used to determine the number of cycles that these components could endure, based on these thermal strains. Beam interruption frequency data from a current accelerator were used to estimate design lifetimes for components. Mitigation options for reducing thermal fatigue are discussed.

I. INTRODUCTION

In the past, accelerator design was focused on maximum particle energy or maximum beam power, rather than on continuous reliable operation for long periods of time. Frequent beam interruptions were tolerated as a price to be paid for maximum particle energy or maximum beam energy. For instance, Table 1 lists the frequency of beam interruptions for the LANSCE accelerator[1]. In the past, power reactors were designed for constant power operation for long periods with no interruptions. The question that will be addressed in this paper is whether these two technologies can be mated successfully. A beam interruption in an accelerator driven system is similar to a reactor scram, but faster. The specific areas addressed in this paper are the thermal fatigue consequences of frequent beam interruptions in an accelerator driven system, and the mitigation options.

Thermal fatigue results have previously been reported[2] for an ALMR[3] type ATW blanket cooled with sodium. There is also considerable interest in lead-bismuth as a coolant for an ATW blanket. Therefore, in this paper the work is extended to a lead-bismuth cooled blanket.

Table 1, Frequency of Beam Interruptions for the LANSCE Accelerator

Duration of interruption	Interruptions per day	Interruptions per year
10 seconds or more	39	14,200
1 minute or more	9.5	3482
5 minutes or more	3.4	1237
15 minutes or more	1.7	617
1 hour or more	.6	214
5 hours or more	.09	34

Figure 1 shows a schematic of the coolant flow in the ALMR mod B design. The coolant flows upward through the core into an outlet plenum. From the outlet plenum the coolant flows directly into the shell side of the intermediate heat exchanger. In the intermediate heat exchanger the primary coolant flows downward and then out into a cold pool. From the cold pool the coolant is drawn into a pump and pumped back into the inlet plenum. The intermediate coolant flows upward through the tubes in the intermediate heat exchanger. It then flows through pipes to the steam generator and back to the intermediate heat exchanger.

For the lead-bismuth cooled blanket design, an attempt was made to come up with a design comparable with the sodium cooled ALMR design, with changes appropriate to the different coolant. The same total blanket power, 840 Mwt, was used for both coolants, as well as the same average core coolant temperature rise, 139 K. Also, the same outlet plenum volume was used. In order to avoid excessive pressure drop through the core for the lead-bismuth design the fuel pin diameter was reduced and the coolant flow area and hydraulic diameter in the core were increased. The intermediate coolant loop was eliminated in the lead-bismuth design, and once-through steam generators were placed inside the primary vessel. Also, to accommodate the extra weight of the lead-bismuth, the reactor vessel wall thickness was increased from two inches to four inches. It should be noted this lead-bisumth design is not a well developed design like the sodium cooled ALMR design. For example, even with the increased vessel wall thickness, this lead-bismuth design may not meet seismic requirements.

Temperature response in the primary coolant system, and in the intermediate coolant system in the case of sodium coolant, was calculated, using the SASSYS-1 systems analysis code[4], for an immediate drop in beam current from full power to zero. Coolant temperatures from SASSYS-1 were fed into a multi-node structure temperature calculation to obtain average temperatures and surface temperatures for the structures. Temperature differences were used to calculate thermal strains. Fatigue curves from the American Society of Mechanical Engineers Boiler and Pressure Vessel Code[5] were used to determine the number of cycles that various components could endure, based on these thermal strains. The beam interruption frequency data of table 1 were used to estimate the design lifetimes for the components.

II. ANALYSIS METHODS

A. The SASSYS-1 Plant Dynamics Code

The SASSYS-1 plant dynamics code contains neutron kinetics coupled with a detailed thermal hydraulics treatment of the core, the primary and intermediate heat removal loops, and the steam generators. Both steady-state and transient calculations are done by the code. The neutron kinetics treatment contains point kinetics, with or without an external source. Also, the neutron kinetics treatment contains an optional 3-D time dependent neutron kinetics capability.

The thermal hydraulics in SASSYS-1 uses a multi-channel treatment for core subassemblies. Each channel represents one subassembly or a group of similar subassemblies. A channel models a fuel pin, its associated coolant, and structure. The subassembly duct wall is treated as structure, and wrapper wires around the fuel pins can be included in the structure. Coolant and structure above and below the fuel pin is also treated: the whole length of the subassembly from the inlet plenum to the outlet plenum is modeled. Beyond the core subassemblies the code calculates coolant pressures and flows, as well as temperatures for coolant and structure (walls). Calculations are made for inlet and outlet plenums, pipes, pumps, intermediate heat exchangers, and steam generators.

B. Program Tslab, One Dimensional Heat Conduction in Slab Geometry

SASSYS-1 calculates structure temperatures, but SASSYS-1 uses only one or two radial nodes in the structure. One or two radial nodes are not sufficient to provide accurate transient temperatures in a transient as fast as those being considered in this work. Therefore, a small, separate code, Tslab, was written to calculate accurate time-dependent structure temperatures, given the coolant temperatures calculated by SASSYS-1.

A convective heat transfer coefficient is used between the coolant temperature and the structure surface temperature. Up to 50 temperature nodes are used within the structure. The structure can consist of a number of separate materials in contact with each other. Thus, when calculating temperatures in the outlet plenum wall, one can include the vessel wall liner, the annulus of stagnant coolant between the wall liner and the vessel wall, and the vessel wall.

C. Program Tcylndr, One Dimensional Heat Conduction in Cylindrical Geometry

In order to calculate temperature profiles within the tube sheets of the steam generators and the intermediate heat exchangers a small program, Tcylndr, was written. The region around a tube penetration through the tube sheet is modelled as a cylinder with an inner radius equal to the inner radius of the tube. The outer radius of the cylinder is chosen to conserve the tube sheet volume associated with one tube. The time-dependent temperatures of the coolant going through the inner hole in the cylinder is taken from the SASSYS-1 calculations. An adiabatic boundary is used at the outer radius of the cylinder. One dimensional radial heat transfer is calculated in the cylinder.

D. Evaluation of Low Cycle Fatigue at Elevated Temperatures

The method used to evaluate low cycle fatigue at elevated temperatures uses an elastic analysis with corrections for creep and plasticity. This method is based on article T-1432 of Appendix T of Subsection NH of the ASME Boiler and Pressure Vessel Code. This type of analysis is required when the temperatures exceed 700 or 800 °F. For a given peak strain and a given peak temperature this method gives the maximum allowable number of cycles that the material can be subjected to.

One problem with the Appendix T treatment is that Appendix T only includes data for four materials: 304 stainless steel, 316 stainless steel, Ni-Fe-Cr alloy 800H, and 2 1/4 Cr-1 Mo steel. In the ALMR design, much of the primary and intermediate coolant loop are made of 304 stainless steel; and the steam generator is made from 2 1/4 Cr-1Mo steel. Any other material, such as the HT-9 used for fuel pin cladding and subassembly duct walls in the ALMR mod B design, is not covered by this treatment. The high silicon martensitic steel recommended by the Russians for use with lead-bismuth coolant is also not covered by this treatment. In contrast, the ASME low cycle fatigue treatment in Subsection NB of section III is limited to temperatures below 700 - 800 °F; but it is applicable to broad classes of steels, including one category for ferritic steels, such as HT-9, and another category for austenitic steels, such as 304 and 316 stainless steel. The fatigue behavior of martensitic steels is probably similar to that of ferritic steels. To estimate fatigue limits for HT-9 at elevated temperatures, it was decided to analyze the load pads with the Appendix T treatment using 316 stainless steel properties and then to multiply the allowable number of cycles by a factor, f_{HT-9}, to get the allowable number of cycles for HT-9. To obtain a value for f_{HT-9} cases were evaluated for both HT-9 and 316 ss using the Section III, Subsection NB treatment and no correction for elevated temperature operation. In these cases the allowable number of cycles for HT-9 tended to be about one sixth of the allowable number of cycles for 316 ss. Thus, the value used for f_{HT-9} is 1/6. The same factor is used for the high silicon martensitic steel used with lead-bismuth coolant.

E. Coolant Heat Transfer Coefficient

An important parameter in the calculation of the thermal strain in the structure is the value used for the coolant heat transfer coefficient at the surface of the structure. For many components, such as the above core load pads, the intermediate heat exchanger shell, the intermediate heat exchanger upper tube sheet rim, and the steam generator upper tube sheet rim, the evaluation of the coolant heat transfer coefficient was straight-forward. A standard forced convection heat transfer correlation was used. On the other hand, for the outlet plenum wall, there is not much forced convection. Therefore, the natural circulation correlation of Churchill and Chu[6] was used for the outlet plenum wall.

III. RESULTS

A. Loss of Beam Transient

Loss of beam transients were run for both the sodium cooled design and the lead-bismuth cooled design. In both cases the initial coolant temperature rise in the hottest core channel was 164 K, and the average coolant temperature rise was 139 K. In these transients, the external source from the beam dropped instantly from full power to zero. The pumps were not tripped. The detailed steam generator model in SAS4A was used in the analysis of these transients. The feed water flow and the turbine throttle valve were adjusted during the transient so as to maintain constant water level in the steam generator and so as to maintain constant steam pressure at the outlet of the steam generator.

Figure 2 shows the powers and flow for the loss of beam transient. At the beginning of a refuelling cycle k effective is about .975, but by the end of the cycle k effective can drop to .92 or lower. It can be seen from Figure 2 that the power drops almost instantly from nominal power to a much lower value after the loss of the beam. Then the power drops slowly toward decay heat levels. In the early part of the transient, the power drops significantly lower with a k effective of .92 rather than .975. The results presented in this section were all run with k effective equal .92. The impact of the degree of subcriticality is discussed in section III B below.

Figure 3 shows the coolant and structure temperatures at the position of the subassembly above core load pads in the hottest subassembly for the lead-bismuth cooled case. During much of the transient, the average structure temperature calculated with 20 radial nodes in TSLAB is about 10 K lower that the value calculated with two radial nodes in SASSYS-1. Figure 4 shows the difference between the structure average temperature and the structure surface temperature at the position of the above core load pads. This difference peaks at 44.6 K at 3.2 seconds into the transient. Results for sodium coolant are similar, except the difference between the structure surface temperature and the coolant temperature is smaller because of the higher thermal conductivity of the sodium. This leads to a larger difference between the structure average temperature and the surface temperature.

Figure 5 shows the coolant and structure temperatures for the upper part of the upper plenum in the lead-bismuth cooled case. The transient involves a much longer time scale in the outlet plenum than in the subassembly because it takes time for the core flow to mix with the large volume of coolant in the outlet plenum. The difference between the coolant temperature and the wall surface temperature is larger than in the subassembly duct wall case because of the lower coolant heat transfer coefficient in the outlet plenum case. Figure 6 shows the difference between the average temperature and the surface temperature for the vessel liner in the outlet plenum. This difference peaks at 27 K at 127 seconds into the transient.

Figure 7 shows the temperatures in the upper tube sheet of the steam generator in the lead-bismuth case. Because of the large diameter of the tubes and the large spacing between tubes, the average temperature in the tube sheet drops slowly even after the temperature of the steam going through the tubes has dropped significantly. The steam temperature drops from its initially superheated value to a temperature near saturation after about 200 seconds into the transient. The tube surface temperature drops to a minimum near 200 seconds then rises. The rise occurs because the steam flow rate drops during the transient, and the steam heat transfer coefficient drops as the flow rate drops. Figure 8 shows the difference between the average tube sheet temperature and the tube surface temperature. This difference peaks at 72.8 at 191 seconds into the transient.

Table 2 summarizes the peak structure temperature differences and gives the corresponding fatigue results for both sodium cooled and lead-bismuth cooled systems. Subassemblies are normally left in the core for three or four years, so with sodium coolant the fatigue damage to the above core load pads is not acceptable unless some mitigation action is taken. With the lead-bismuth design the above core load pads are okay if the frequency of beam interruptions is no worse than the LANSCE data. With either coolant the damage to the vessel liner and to the vessel wall is within acceptable bounds with the specified frequency of interruptions. If the plant is expected to operate for 30 years, then the fatigue damage to the intermediate heat exchanger tube sheet rim in the sodium cooled case, and to the steam generator tube sheet in the lead-bismuth cooled case, require mitigation action. The largest uncertainty in these calculations is the actual frequency of interruptions of the accelerator. The ATW accelerator has not been designed or built, so the actual reliability of the beam is unknown.

It might appear from the results in Table 3 that from a thermal fatigue point of view lead-bismuth is a better coolant for the ATW design than sodium, but out of necessity the designs are different. In particular, in order to avoid a large coolant pressure drop in the core, the lead-bismuth design uses smaller pins with more space between pins. If the sodium cooled design used the same small pins and larger space between pins, then for the same pumping power the sodium cooled device could have a significantly higher coolant flow rate, leading to a smaller coolant temperature rise across the core and significantly

Table 2, Estimates of Fatigue Damage Due to Beam Interruptions

structural element	coolant	material	thickness (m)	peak ΔT (K)	time of peak (s)	allowable cycles	interruptions /year	years of operation
above core load pads	Pb-Bi	martinsitic	.0056495	44.6	3.2	6.8×10^4	14,200	4.8
	Na	HT-9	.0056495	66.2	1.9	7517	14,200	.53
outlet plenum upper wall	Pb-Bi	martinsitic	.0254	27.0	127	1.7×10^5	2230	75+
	Na	304 ss	.0254	40.7	121	10^6+	2230	450+
IHX tube sheet rim	Na	304 ss	.0635	114.3	219	2475	1556	1.6
steam generator tube sheet	Pb-Bi	martensitic	.0753	72.8	191	8100	1648	4.9
	Na	2 1/4cr-1 Mo	.0753	68.3	211	2.6×10^5	1556	167

lower thermal strains in the transient.

B. Impact of the Degree of Sub-Criticality

As mentioned previously, the results in the previous section were run with a blanket k effective of .92, which is typical of the value at the end of a re-fuelling cycle, whereas at the beginning of the cycle k effective might be .975. Therefore, one case was run with a k effective of .975. This was a sodium cooled case identical to the case previously described except for the value of k effective. Figure 9 shows the influence of k effective on the difference between the above core load pad average temperature and the structure surface temperature at this location. With k effective equal to .975, the peak temperature difference is 62.2 K instead of 66.2. This is not a large difference, but the fatigue curves are very non-linear. The difference of 4.0 K in peak temperature difference results in almost doubling the allowable number of cycles, from 7500 to 12,000. Downstream of the core subassemblies, in the outlet plenum and beyond, the transient temperature changes caused by changing k effective from .92 to .975 are less than 1 K. Thus, the main fatigue consequence is in the subassemblies.

IV. MITIGATION OPTIONS

A number of mitigation options can be considered to solve thermal fatigue problems. These mitigation options tend to fall in one of two categories. One category is reducing the frequency of beam interruptions. The second category is to reduce the amplitude of the temperature perturbations.

A. Improve the Reliability of the Accelerator

Improving the reliability of the accelerator and reducing the frequency of beam interruptions would extend the lifetime of components subjected to thermal fatigue. Improving the reliability of the accelerator would also improve the average effective utilization of the ATW, increasing the rate at which waste is transmuted and increasing the amount of electricity produced. Using multiple accelerators, with each providing a fraction of the required beam current is another solution. If two accelerators were used, with each providing half of the beam current, then losing one accelerator beam would only cut the blanket power in half. The amplitude of the thermal strain cycle would be cut in half. The frequency of interruptions might be doubled; but because of the non-linearity of the fatigue curves, the allowable number or cycles would be increased by an order of magnitude or more.

B. Pump Trip

In a critical reactor, the pumps are normally tripped when a scram occurs. This is to limit thermal shock in various structures. In an ATW the pumps and turbines could be tripped whenever a beam interruption occurs. This would largely eliminate thermal fatigue problems associated with beam interruptions.

There are two problems with tripping the pumps and turbines every time a beam interruption occurs in an ATW. One problem is a safety problem, and the other problem relates to the average load factor or utilization. If one trips the pumps a few hundred thousand times during the lifetime of a plant, then the probability is fairly high that sometime the beam will be lost, the pumps will be tripped, the beam will be restored, but the pumps will not be restarted. This results in an accident equivalent to a loss-of-flow accident. The ALMR reactor was designed to survive a loss-of-flow accident, with negative reactivity feedback reducing the power to a level that natural circulation flow could handle. In the ATW, negative reactivity feedback has little impact on the power level. Thus in a sodium cooled ATW, a loss-of-flow accident would lead to a core meltdown. For the lead-bismuth cooled reactor design considered here, there would be enough natural circulation flow that core melting would not occur.

The average load factor or utilization problem comes about because every time that the turbines are tripped, it takes many hours to bring them back on-line. If there is a beam interruption, followed by a pump trip and a turbine trip, every half hour or so of operation, followed by a number of hours restarting the turbines, then the device is not going to be operating very much of the time.

C. Reducing the Core Coolant Temperature Rise

If the frequency of beam interruptions can not be reduced sufficiently, and if a single accelerator is to be used, then probably the most feasible way to reduce the thermal fatigue to an acceptable level is to reduce the core coolant temperature rise by increasing the coolant flow rate or by reducing the power per fuel pin. It may also be necessary to limit the amount of superheat in the once-through steam generator. The temperature differences driving thermal fatigue effects in all structures from the core to the steam generator inlet are proportional to the core temperature rise. The temperature differences in the upper tube sheet of the steam generator are mainly proportional to the steam superheat. Because of the highly non-linear nature of the fatigue curves, relatively small reductions in core coolant temperature rise and in steam generator superheat may be sufficient.

V. CONCLUSIONS

Beam interruption frequencies typical of the LANSCE accelerator can lead to serious thermal fatigue problems in either a lead-bismuth cooled or a sodium cooled ATW blanket. Mitigation options exist, but they can be costly.

ACKNOWLEDGMENTS

This work was supported by the U.S. Department of Energy under Contract No. W-31-109-ENG-38.

REFERENCES

1. W. Gudowski, DOE Expert Panel for the ATW, Washington DC (February 1999).

2. F. E. Dunn, "Thermal Fatigue Due to Beam Interruptions for an ALMR-Type ATW," *Trans. Am . Nucl. Soc.* **82**, 258 (2000)..

3. P. M. Magee, A. E. Dubberley, A. J. Lipps and T. Wu, "Safety Performance of the Advanced Liquid Metal Reactor," *Proceedings of ARS '94 International Topical Meeting on Advanced Reactors Safety*, Pittsburg, Pennsylvaina, Vol. 2, pp. 826-833 (April 1994)..

4. F. E. Dunn, F. G. Prohammer, D. P. Weber and R. B. Vilim, "The SASSYS-1 LMMFBR Systems Analysis Code," *ANS International Topical Meeting on Fast Reactor Safety*, Knoxville, TN, pp. 999-1006 (April 1985).

5. The American Society of Mechanical Engineers, *1998 ASME Boiler & Pressure Vessel Code, an International Code*, Section III, Subsection NH, Appendix T, Article T-1432.

6. S. W. Chruchill and H. H. S. Chu, "Correlating Equations for Laminar and Turbulent Free Convection from a Vertical Plate," *Int. J. Heat Mass Transfer*, Vol. 18, pp. 1323-1329, 1975.

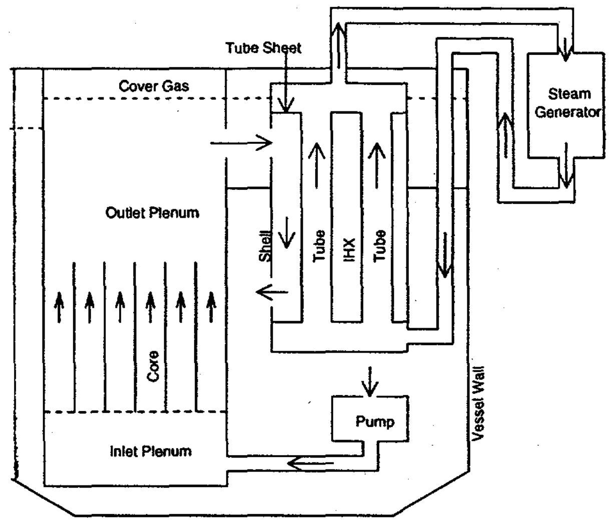

Fig. 1, Schematic of Coolant Flow in the ATW Blanket

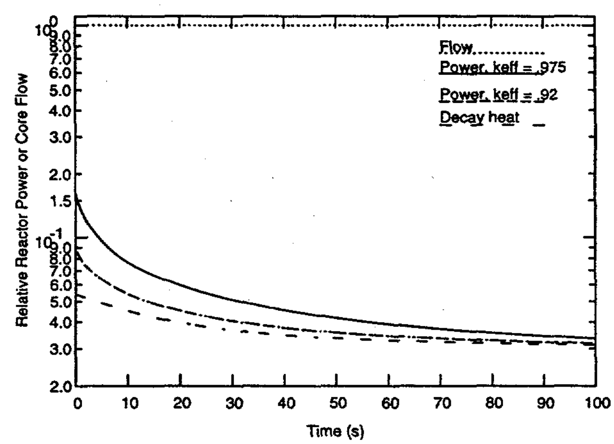

Fig. 2, Normalized Power and Flow for a Beam Loss

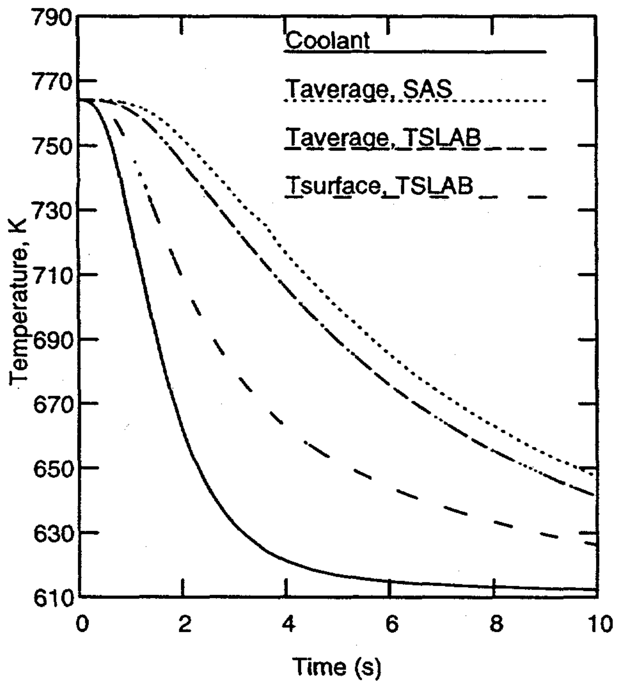

Fig. 3, Top of Core Coolant and Structure Temperatures

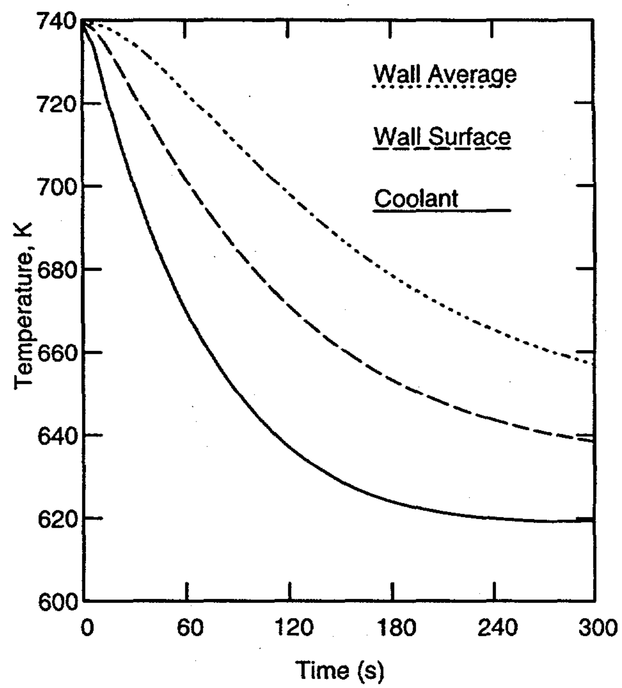

Fig. 5. Outlet Plenum Temperatures

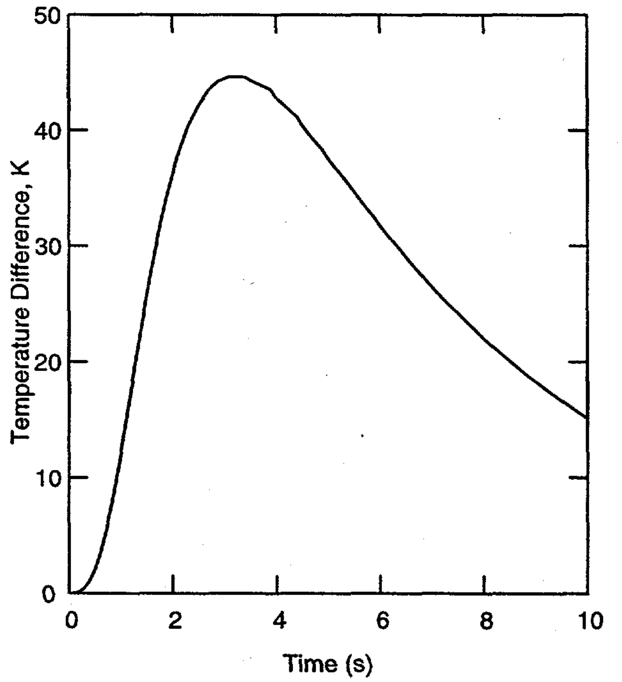

Fig. 4, Top of Core Structure Average Temperature - Surface Temperature

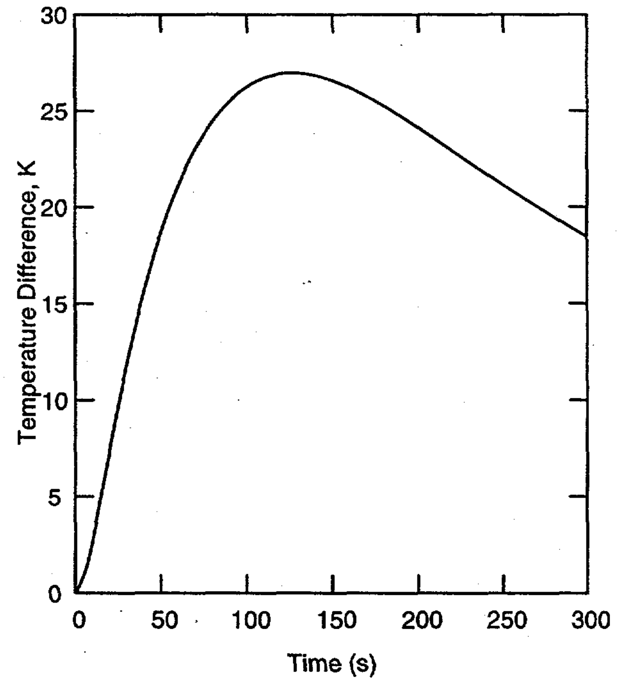

Fig. 6, Outlet Plenum Structure Average Temperature - Surface Temperature

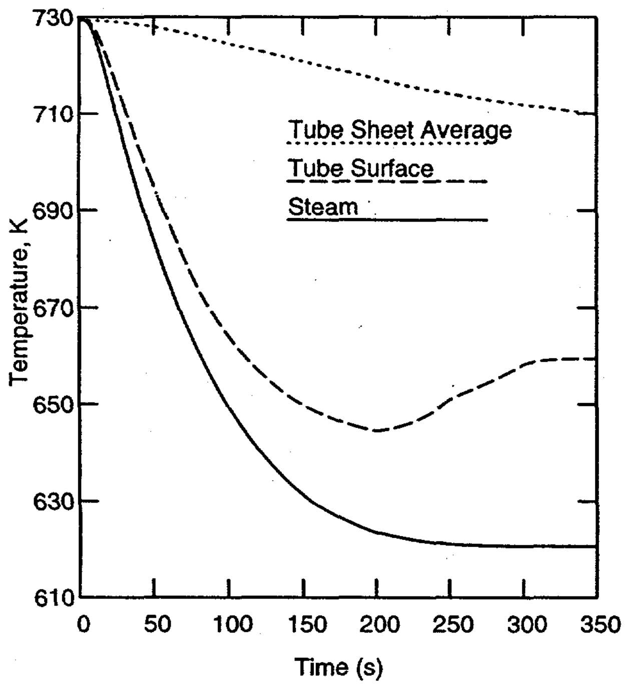

Fig. 7, Steam Generator Upper Tube Sheet Temperatures

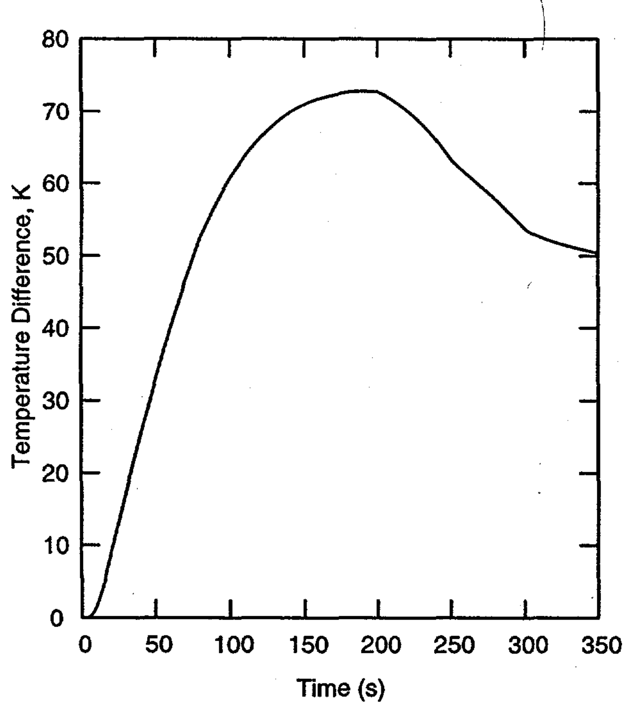

Fig. 8, Steam Generator Tube Sheet Average Temperature - Tube Surface Temperature

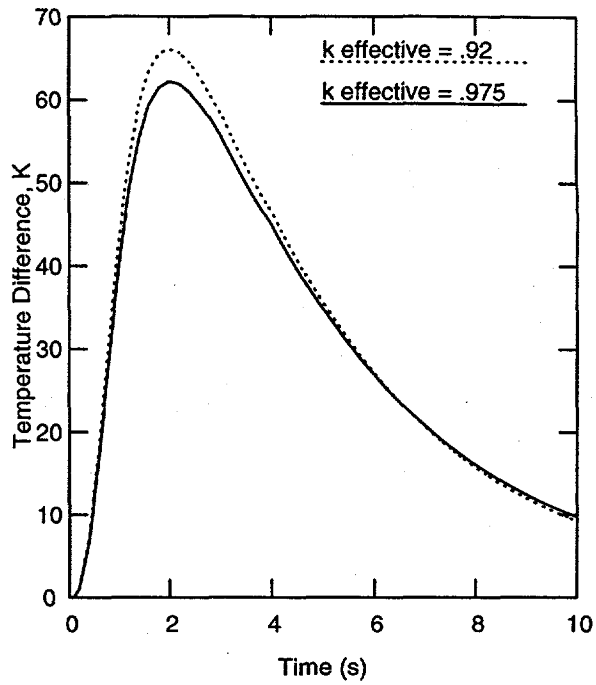

Fig. 9, Influence of K Effective on the Difference Between Top of Core Structure Average Temperature and Surface Temperature